Muthu and Raja *Journal of the European Optical Society-Rapid Publications* (2016) 12:24
DOI 10.1186/s41476-016-0028-2

Journal of the European Optical Society-Rapid Publications

RESEARCH Open Access

Bidirectional MM-Wave Radio over Fiber transmission through frequency dual 16-tupling of RF local oscillator

K. Esakki Muthu[1*] and A. Sivanantha Raja[2]

Abstract

In this paper for the first time, a 60 GHz bidirectional Millimeter Wave (MM-Wave) Radio over Fiber (RoF) transmission through a new frequency dual 16-tupling of 3.75 GHz local oscillator (LO) is demonstrated. The proposed system is constructed with parallel combination of two cascaded stages of MZMs. The upper cascaded stage and the Lower cascaded stages are biased at the Maximum Transmission Point (MATP). By suitable adjustments of LO phase and amplitude, optical sidebands with spacing of 8 times the input LO frequency is generated. These sidebands are then separated using filters to achieve dual 16-tupling. A good agreement between numerical derivations and the simulation results are achieved. Further, a simulation is performed to access the dual bidirectional transmission performance for the double and single tone modulation with 2.5 Gbps data transmission. The transmission distance is limited to 25 km for the double tone modulation due to bit walk of effect. A 60 km link distance is achieved with single tone modulation. The dispersion induced power penalties less than 0. 5 dB at 10^{-9} BER is observed for both up and down streams.

Keywords: Millimeter Wave, 16-tupling, Radio over Fiber, Mach-Zehnder Modulator

Background

From the past two decades demands for the high data rate wireless services are ever increasing. To support such a growing demand, a higher bandwidth carrier frequency is required. As the lower frequency spectrum up to 30 GHz is congested, the MM-Wave band (30–300GHz) is now considered to be the promising candidate for the support of the emerging data traffic since it offers 270 GHz bandwidth. Though, a major bottle neck of the MM-Wave communications are the MM-Wave generation and transmission since the electrical generation suffers from the limited frequency response of the available conventional electronics components and, the MM-Wave transmission suffers from huge free space/cable losses [1]. A viable solution for this issue enables us to use the hybrid system which combines both wireless and optical communications, where the MM-Waves are generated by optical methods at the central station (CS) and distributed over an optical fiber to the base station (BS). The optical generation and distribution of MM-Wave enjoys the low loss and huge bandwidth of the optical fibers. Several optical MM-Wave generation methods have been proposed including direct modulation of the laser diode, optical heterodyning of the highly correlated laser sources and external modulation. Among these, external modulation based frequency multiplication techniques have become popular due to higher modulation bandwidth, tunability and high stability [2, 3]. Several multiplication techniques have been proposed with different multiplication factors such as doubling [3], tripling [4], quadrupling [5–7], sextupling [8], octupling [9], 12-tupling [10], 16- tupling [11, 12] and so on. A MM-Wave generation technique with highest frequency multiplication factor reduces the need of high frequency RF local oscillator at the CS. However, cost effective design of CS as well as the BS is a challenge. A full duplex RoF system which shares a single laser source is a one of the cost effective techniques. In addition to this, reduction of high frequency RF LO at the CS will bring down the cost of the entire system. Hence, a full duplex RoF transmission with frequency dual quadrupling was proposed in [13], dual sextupling [14] and dual octupling presented in [15] these methods were using

* Correspondence: esaionly@gmail.com
[1]University VOC College of Engineering, University VOC, Thoothukudi, Tamilnadu 630003, India
Full list of author information is available at the end of the article

a single laser source for both upstream and downstream by supporting two BSs simultaneously. However, as the frequency multiplication factor is too low, there is a demand for a high frequency RF local oscillator at the CS. To achieve a higher frequency multiplication factor, two or more MZMs were employed either in series or in parallel configuration. A cascaded combination of two MZMs was used to generate frequency quadrupling [16], sextupling [8, 17] and octupling [18]. Three arm MZM was used for the generation of sextupling in [19] and three parallel MZMs were used to generate sextupling, 12-tupling and 18 tupling in [20]. A frequency octupling was generated using 4 MZMs in [21, 22].

In this paper, we propose a novel frequency dual 16-tupling of the given RF local oscillator which will considerably eliminate the need for a high frequency RF local oscillators at the CS compared to the other techniques proposed in [13, 15] and also as it supports full duplex transmission by wavelength reuse, cost of both CS and BS can be greatly minimized. A mathematical proof of the proposed scheme is presented and for the proof of concept a simulation is conducted with full bidirectional MM-W RoF transmission.

The structure of this paper is as follows, the mathematical principle behind the proposed technique is discussed in the section II. The simulation work and results of proposed scheme is presented in section III and finally, conclusion is presented in the chapter IV.

Principle

The principle behind the proposed scheme is depicted in Fig. 1. The proposed configuration is composed of parallel combination of two cascaded MZMs. A CW DFB laser source $E_o(t) = E_o cos\omega_c t$ drives the both upper and the lower cascaded stages of the MZMs. The upper cascaded stage consists of MZM1 and MZM2 and the lower cascaded stage consists of MZM3 and MZM4, they are all biased at its Maximum Transmission Point (MATP).

The both the electrodes of the MZM1 is driven by $v_1(t) = V_{rf} \sin \omega_m t$, and the transfer function of the MZM1 can be expressed as,

$$E_{MZM1}(t) = \frac{E_o}{4} cos\omega_c t \left[e^{j\frac{\pi V_{rf}}{V_\pi} \sin(\omega_m t) + j\frac{\pi V_{b2}}{V_\pi}} + e^{-j\frac{\pi V_{rf}}{V_\pi} \sin(\omega_m t) + j\frac{\pi V_{b1}}{V_\pi}} \right] \quad (1)$$

where V_{rf} is the RF signal amplitude, V_π is the switching bias voltage of the MZM, V_{b1} and V_{b2} are the bias voltage of the electrodes, by setting $V_{b1} = V_{b2} = V_\pi/2$, the Eq. (1) can be rewritten as,

$$E_{MZM1}(t) = \frac{E_o}{4} cos\omega_c t \left[j\left(e^{jm \sin(\omega_m t)} + e^{-m \sin(\omega_m t)} \right) \right] \quad (2)$$

where $m = \pi V_{rf}/V_\pi$ is the modulation index. Using the Bessel function of first kind the Eq. (2) can be written as,

$$E_{MZM1}(t) = j\frac{E_o}{2} cos\omega_c t \left[\left(J_0(m) + 2\sum_{n=1}^{\infty} J_{2n}(m) cos 2n\omega_m t \right) \right] \quad (3)$$

where J(.) is the Bessel function of order n. The Eq. (2) shows that the output of MZM1 contains even order sidebands along with central carrier. And the electrodes of the MZM2 are driven by $v_2(t) = V_{rf} \sin\left(\omega_m t + \frac{\pi}{2}\right)$, the transfer function of the MZM2 can be expressed as

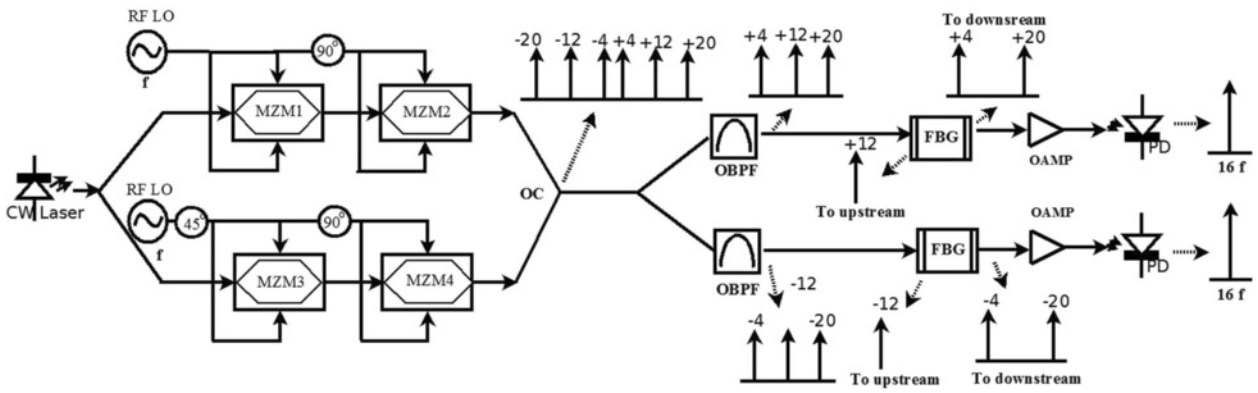

Fig. 1 Schematic of the proposed system CW: Continuous Wave; MZM: Mach-Zehnder Modulator; OBPF: Optical Band Pass Filter; FBG: Fiber Bragg Grating; OAMP: Optical Amplifier; PD: Photo detector

$$E_{MZM2}(t) = j\frac{E_o}{4}cos\omega_c t\left[\left(e^{jm\sin\left(\omega_m t+\frac{\pi}{2}\right)} + e^{-m\sin\left(\omega_m t+\frac{\pi}{2}\right)}\right)\right] \tag{4}$$

Using Bessel function,

$$E_{MZM2}(t) = \mathrm{j}\left[\left(\mathrm{J}_0(\mathrm{m}) + \sum_{\mathrm{n}=1}^{\infty}(-1)^{\mathrm{n}}\mathrm{J}_{2\mathrm{n}}(\mathrm{m})cos2n\omega_m t\right)\right] \tag{5}$$

Then the output of the upper cascaded stage can be expressed as,

$$E_U(t) = E_{MZM1}(t) * E_{MZM2}(t) \tag{6}$$

$$E_U(t) = -\frac{E_o}{2}cos\omega_c t\left\{\left[\mathrm{J}_0(\mathrm{m}) + 2\sum_{\mathrm{n}=1}^{\infty}\mathrm{J}_{2\mathrm{n}}(\mathrm{m})\cos(2n\omega_m t)\right] * \left[\mathrm{J}_0(\mathrm{m}) + 2\sum_{\mathrm{n}=1}^{\infty}(-1)^{\mathrm{n}}\mathrm{J}_{2\mathrm{n}}(\mathrm{m})^2\cos(2n\omega_m t)\right]\right\} \tag{7}$$

By eliminating common terms and higher order terms whose magnitudes are very low, the Eq. (7) can be reduced to,

$$E_U(t) = -\frac{E_o}{2}cos\omega_c t\{\mathrm{J}_0{}^2(\mathrm{m}) + 2\mathrm{J}_0(\mathrm{m})\sum_{\mathrm{n}=1}^{\infty}(-1)^{\mathrm{n}}\mathrm{J}_{2\mathrm{n}}(\mathrm{m})\cos(2n\omega_m t)) + 2\mathrm{J}_0(\mathrm{m})\sum_{\mathrm{n}=1}^{\infty}\mathrm{J}_{2\mathrm{n}}(\mathrm{m})\cos(2n\omega_m t) + 2\mathrm{J}_0(\mathrm{m})\left[\sum_{n=1}^{\infty}(-1)^{n}\mathrm{J}_{2\mathrm{n}}{}^2(\mathrm{m})\{1+\cos(4n\omega_m t)\}\right]\} \tag{8}$$

Simplification of the above eqn. results,

$$\begin{aligned}E_U(t) = \frac{E_o}{2}cos\omega_c t\{&-\mathrm{J}_0{}^2(\mathrm{m}) + \mathrm{J}_2{}^2(\mathrm{m}) + \mathrm{J}_2{}^2(\mathrm{m})cos4\omega_m t\\ &+ 4\mathrm{J}_0\mathrm{J}_4\,(\mathrm{m})cos4\omega_m t - 2\mathrm{J}_4{}^2(\mathrm{m}) - 2\mathrm{J}_4{}^2(\mathrm{m})cos8\omega_m t\\ &+ 2\mathrm{J}_6{}^2(\mathrm{m}) + 2\mathrm{J}_6{}^2(\mathrm{m})cos12\omega_m t - 4\mathrm{J}_0\mathrm{J}_8\,(\mathrm{m})cos8\omega_m t\\ &- 2\mathrm{J}_8{}^2(\mathrm{m}) - 2\mathrm{J}_8{}^2(\mathrm{m})\cos8\omega_{\mathrm{m}} t + 2\mathrm{J}_{10}{}^2(\mathrm{m})\\ &+ \mathrm{J}_{10}{}^2(\mathrm{m}) + 2\mathrm{J}_{10}{}^2(\mathrm{m})cos20\omega_m t - 4\mathrm{J}_0\mathrm{J}_{12}\,(\mathrm{m})cos12\omega_m t\\ &- 2\mathrm{J}_{12}{}^2(\mathrm{m}) - 2\mathrm{J}_{12}{}^2(\mathrm{m})cos24\omega_m t + \mathrm{J}_{14}{}^2(\mathrm{m})\\ &+ 2\mathrm{J}_{14}{}^2(\mathrm{m})cos28\omega_m t - 4\mathrm{J}_0\mathrm{J}_{16}\,(\mathrm{m})cos16\omega_m t - 2\mathrm{J}_{16}{}^2(\mathrm{m})\\ &- 2\mathrm{J}_{16}{}^2(\mathrm{m})cos32\omega_m t - 2\mathrm{J}_{18}{}^2(\mathrm{m})\\ &- 2\mathrm{J}_{18}{}^2(\mathrm{m})cos36\omega_m t - 4\mathrm{J}_0\mathrm{J}_{20}\,(\mathrm{m})cos20\omega_m t\\ &- 2\mathrm{J}_{20}{}^2(\mathrm{m}) - 2\mathrm{J}_{20}{}^2(\mathrm{m})cos40\omega_m t - \cdots\}\end{aligned} \tag{9}$$

From Eq. (9) one can observe that output of the upper cascaded stage consists sidebands which are integer multiples of four. In the lower cascaded stage can output of the MZM3 is driven by $v_3(t) = V_{rf}\sin\left(\omega_m t + \frac{\pi}{4}\right)$, and setting $V_{b1} = V_{b2} = 0$, the transfer function of the MZM3 can be written as be written as,

$$E_{MZM3}(t) = \frac{E_o}{4}cos\omega_c t\left[\begin{matrix}e^{jm\sin\left(\omega_m t+\frac{\pi}{4}\right)}\\ +e^{-m\sin\left(\omega_m t+\frac{\pi}{4}\right)}\end{matrix}\right] \tag{10}$$

Using Bessel function of first kind,

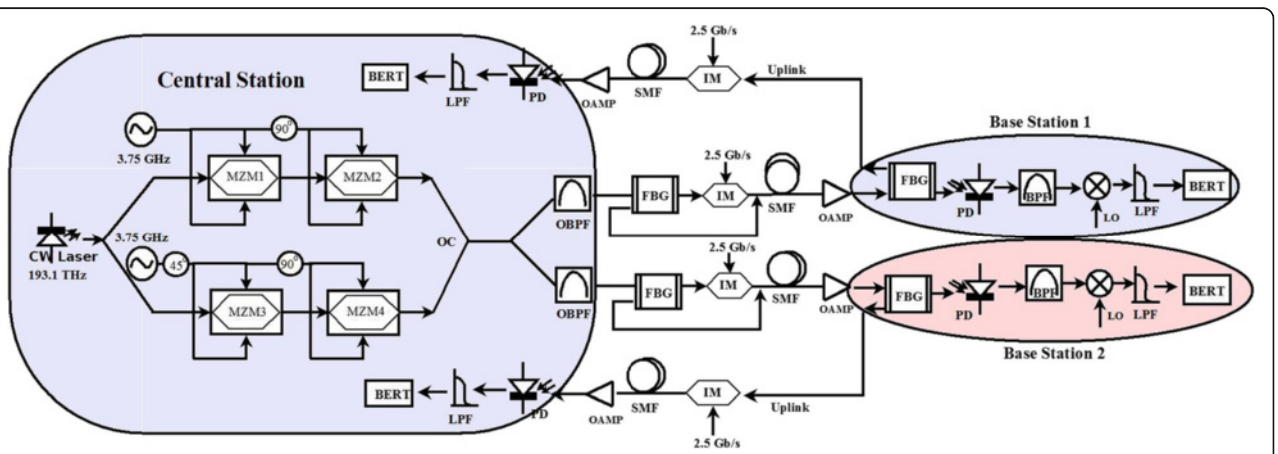

Fig. 2 Simulation setup. CW: Continuous Wave; MZM: Mach-Zehnder Modulator; OBPF: Optical Band Pass Filter; FBG: Fiber Bragg Grating; IM: Intensity Modulator; SMF: Single Mode Fiber; OAMP: Optical Amplifier; PD: Photo detector; BPF: Band Pass Filter; LPF: Low Pass Filter; LO: Local Oscillator; BERT: Bit Error Rate Tester

$$E_{MZM3}(t) = \frac{E_o}{2} cos\omega_c t \left[\begin{matrix} \mathrm{J_0(m)+} \\ 2\sum_{\mathrm{n=1}}^{\infty} \mathrm{J_{2n}(m)} cos2n(\omega_m t + \pi/4) \end{matrix} \right] \tag{11}$$

The output of the MZM4 driven by the $v_4(t) = V_{rf} \sin\left(\omega_m t + \frac{3\pi}{4}\right)$ and setting $V_{b1} = V_{b2} = 0$ can be written as,

$$E_{MZM4}(t) = \frac{E_o}{4} cos\omega_c t \left[\begin{matrix} e^{jm \sin\left(\omega_m t + \frac{3\pi}{4}\right)} \\ +e^{-jm \sin\left(\omega_m t + \frac{3\pi}{4}\right)} \end{matrix} \right] \tag{12}$$

Using Bessel function,

$$E_{MZM4}(t) = \left[\mathrm{J_0(m)} + 2\sum_{\mathrm{n=1}}^{\infty} (-1)^{\mathrm{n}} \mathrm{J_{2n}(m)} cos2n\left(\omega_m t + \frac{\pi}{4}\right) \right] \tag{13}$$

Hence the output of the lower cascaded stage can be expressed as,

$$E_L(t) = E_{MZM3}(t) * E_{MZM4}(t) \tag{14}$$

$$\begin{aligned} E_{LI}(t) = \frac{E_o}{2} cos\omega_c t \Big\{ & \mathrm{J_0{}^2(m)} + 2\mathrm{J_0(m)} \sum_{\mathrm{n=1}}^{\infty} (-1)^{\mathrm{n}} \mathrm{J_{2n}(m)} \cos 2n\left(\omega_m t + \frac{\pi}{4}\right) \\ & + 2\mathrm{J_0(m)} \sum_{\mathrm{n=1}}^{\infty} \mathrm{J_{2n}(m)} \cos 2n\left(\omega_m t + \frac{\pi}{4}\right) \\ & + 2\mathrm{J_0(m)} \left[\sum_{n=1}^{\infty} (-1)^{n} \mathrm{J_{2n}{}^2(m)} \left\{ 1 + \cos 4n\left(\omega_m t + \frac{\pi}{4}\right) \right] \right\} \end{aligned} \tag{15}$$

Simplification of the above eqn. results,

$$\begin{aligned} E_L(t) = \frac{E_o}{2} cos\omega_c t \{ & \mathrm{J_0{}^2(m) - J_2{}^2(m) - J_2{}^2(m)} cos(4\omega_m t + \pi) \\ & + 4\mathrm{J_0J_4\ (m)} cos(4\omega_m t + \pi) + 2\mathrm{J_4{}^2(m)} + 2\mathrm{J_4{}^2(m)} cos(8\omega_m t + 2\pi) \\ & - 2\mathrm{J_6{}^2(m) - 2J_6{}^2(m)} cos(12\omega_m t + 3\pi) - 4\mathrm{J_0J_8\ (m)} (cos8\omega_m t + 2\pi) \\ & + 2\mathrm{J_8{}^2(m)} + 2\mathrm{J_8{}^2(m)} \cos(16\omega_m t + 4\pi) - 2\mathrm{J_{10}{}^2(m)} \\ & - 2\mathrm{J_{10}{}^2(m)} cos(20\omega_m t + 5\pi) - 4\mathrm{J_0J_{12}\ (m)} cos12\omega_m t + 3\pi) \\ & + 2\mathrm{J_{12}{}^2(m)} + 2\mathrm{J_{12}{}^2(m)} cos(24\omega_m t + 6\pi) - \mathrm{J_{14}{}^2(m)} \\ & - 2\mathrm{J_{14}{}^2(m)} cos(28\omega_m t + 7\pi) \\ & - 4\mathrm{J_0J_{16}\ (m)} cos(16\omega_m t + 4\pi) + 2\mathrm{J_{16}{}^2(m)} \\ & + 2\mathrm{J_{16}{}^2(m)} \cos(32\omega_m t + 8\pi) - 2\mathrm{J_{18}{}^2(m)} \\ & - 2\mathrm{J_{18}{}^2(m)} cos(36\omega_m t + 9\pi) \\ & - 4\mathrm{J_0J_{20}\ (m)} cos(20\omega_m t + 5\pi) + 2\mathrm{J_{20}{}^2(m)} \\ & + 2\mathrm{J_{20}{}^2(m)} cos(40\omega_m t + 10\pi) - \cdots \} \end{aligned} \tag{16}$$

The resultant optical output after the optical coupler can be expressed as,

$$E_O(t) = E_{LI}(t) + E_L(t) \tag{17}$$

Cancelling the terms which are integer multiples of eight and eliminating the higher order terms due to its low power, the Eq. (18) can be expressed as,

$$\begin{aligned} E_O(t) = \frac{E_o}{2} cos\omega_c t \Big\{ & \left[4\mathrm{J_2{}^2(m)} - 8\mathrm{J_0J_4\ (m)} \right] cos4\omega_m(t) \\ & + \left[4\mathrm{J_6{}^2(m)} - 8\mathrm{J_0J_{12}\ (m)} \right] cos12\omega_m t \\ & + \left[4\mathrm{J_{10}{}^2(m)} - 8\mathrm{J_0J_{20}\ (m)} \right] cos20\omega_m t \Big\} \end{aligned} \tag{18}$$

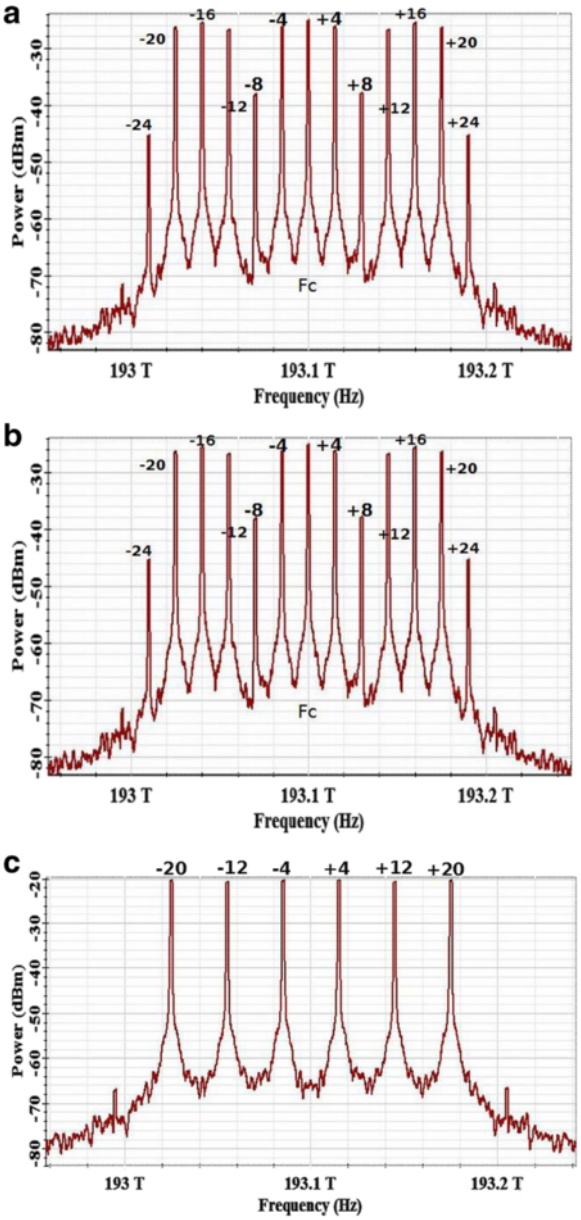

Fig. 3 Spectra after various test locations (**a**) output of the upper cascaded Stage (**b**) output of the Lower cascaded Stage (**c**) Output of the optical coupler

The Eq. (18) clearly shows that there are only ($\omega_c \pm 4\omega_c$), ($\omega_c \pm 8\omega_c$), ($\omega_c + 12\omega_c$), and ($\omega_c + 20\omega_c$) order sidebands. For want of dual 16-tupling the upper sidebands ($\omega_c + 4\omega_c$), ($\omega_c + 12\omega_c$) and ($\omega_c + 20\omega_c$) should be separated and then only ($\omega_c + 4\omega_c$) and ($\omega_c + 20\omega_c$) sidebands will be allowed to beat at the photo detector to result a MM-Wave frequency output which is 16 time the input local oscillator frequency. At the same time, the sideband corresponding to the ($\omega_c + 12\omega_c$) will be reused by the BS1 for the uplink data transmission. Similarly, the lower sidebands ($\omega_c - 4\omega_c$) and ($\omega_c - 20\omega_c$) sidebands will be beating at the photo detector to generate 16 tupled MM-Wave and the sideband ($\omega_c - 12\omega_c$) will be reused at the BS2 for the uplink transmission. Hence, along with dual 16 tupled MM-Wave generation, a bidirectional MM-Wave RoF communication can also be established between the CS and BS.

Simulation, Results and Discussions

A simulation setup used for the verification of the proposed system is shown in Fig. 2. A 10 MHz spectral width continuous wave (CW) laser source with 193.1 THz central frequency is split equally and launched in to the upper and lower cascaded stages of this configuration. Both the MZMs in the upper cascaded stage and the lower stages are biased at its MATP with switching bias voltage of 4 V. The upper stage has two cascaded MZMs (MZM1 and MZM2). In this, the MZM1 is driven by 3.75 GHz Radio Frequency Local Oscillator (RF LO) and the MZM2 is driven by the same LO with 90° phase shift. Bias voltage V_{b1} and V_{b2} are set to 2 V for the upper cascaded stage. The lower stage has two cascaded MZMs (MZM3 and MZM4). The MZM3 is driven by a LO with 45° phase shift and the MZM4 is driven by LO with 135° phase shift. Amplitude of all the RF LOs are set to 4 V. The bias voltage of the lower cascaded stage is set to zero and the extinction ratios of all the MZMs are set to 100 dB. As both the MZMs in the upper cascaded stage is biased at MATP, the output of the upper cascaded stage has sidebands which are integer multiples of four along with the carrier as shown in Fig. 3(a). The output of the lower cascaded stage is shown in Fig. 3(b). It contains similar sideband, but the carrier (ω_c) and sidebands which are integer multiples of 4 such as ($\omega_c \pm 8\omega_c$), ($\omega_c \pm 16\omega_c$) and ($\omega_c \pm 24\omega_c$) are exactly out of phase with the upper cascaded stage. Then the output of the upper and lower cascaded stages are combined using an optical coupler. The coupler output shown in Fig. 3(c), it shows only the in-phase components such as, ($\omega_c \pm 4\omega_c$), ($\omega_c \pm 12\omega_c$) and ($\omega_c \pm 20\omega_c$). Further, the coupler output is equally split and then, the upper sidebands ($\omega_c + 4\omega_c$), i.e., 193.115 THz, ($\omega_c + 12\omega_c$) i.e., 193.145 THz and ($\omega_c + 20\omega_c$) i.e., 193.175 THz are separated utilizing an optical band pass filter (OBPF) with 193.145 THz central frequency and 100 GHz bandwidth, similarly the lower sidebands ($\omega_c - 4\omega_c$) i.e., 193.085 THz,

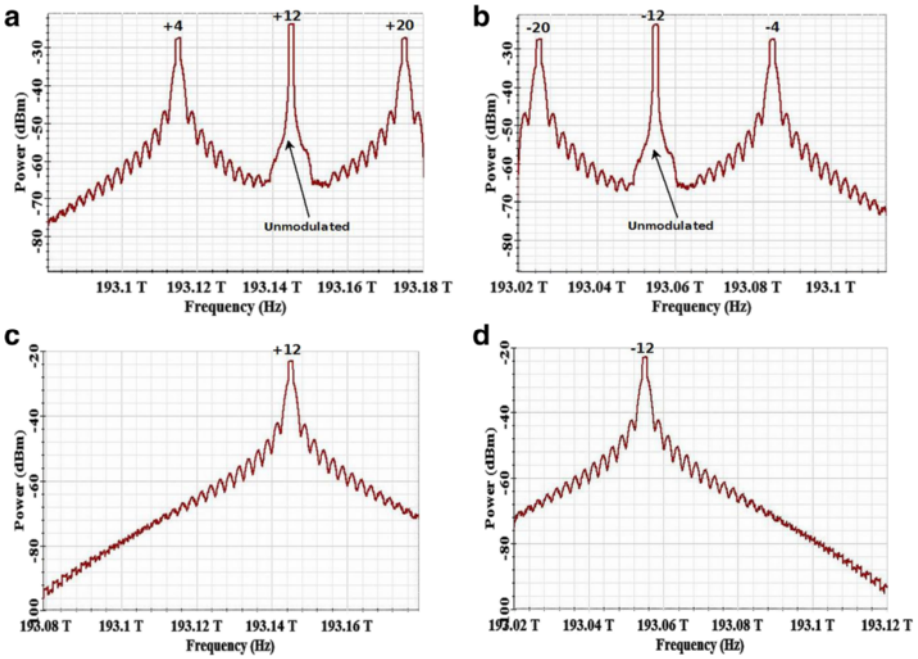

Fig. 4 Spectra after various test locations (**a**) Downstream data modulation on +4th and +20th order sidebands from CS to BS1 (**b**) Downstream data modulation on −4th and −20th order sidebands from CS at BS2 (**c**) Upstream data modulation on +12th order sideband from BS1 to CS (**d**)) Upstream data modulation on −12th order sideband from BS1to CS

$(\omega_c - 12\omega_c)$ i.e., 193.055 THz and $(\omega_c - 20\omega_c)$ i.e., 193.025 THz are separated using an OBPF with a central frequency of 193.055 THz and bandwidth of 100 GHz bandwidth. In the upper sidebands, +12th order sideband (195.145 THz) is reflected using a Fiber Bragg Grating (FBG) with the bandwidth of 10 GHz and now we can see that the remaining +4th (193.115 THz) and +20th (193.175 THz) order sidebands are differ by the frequency

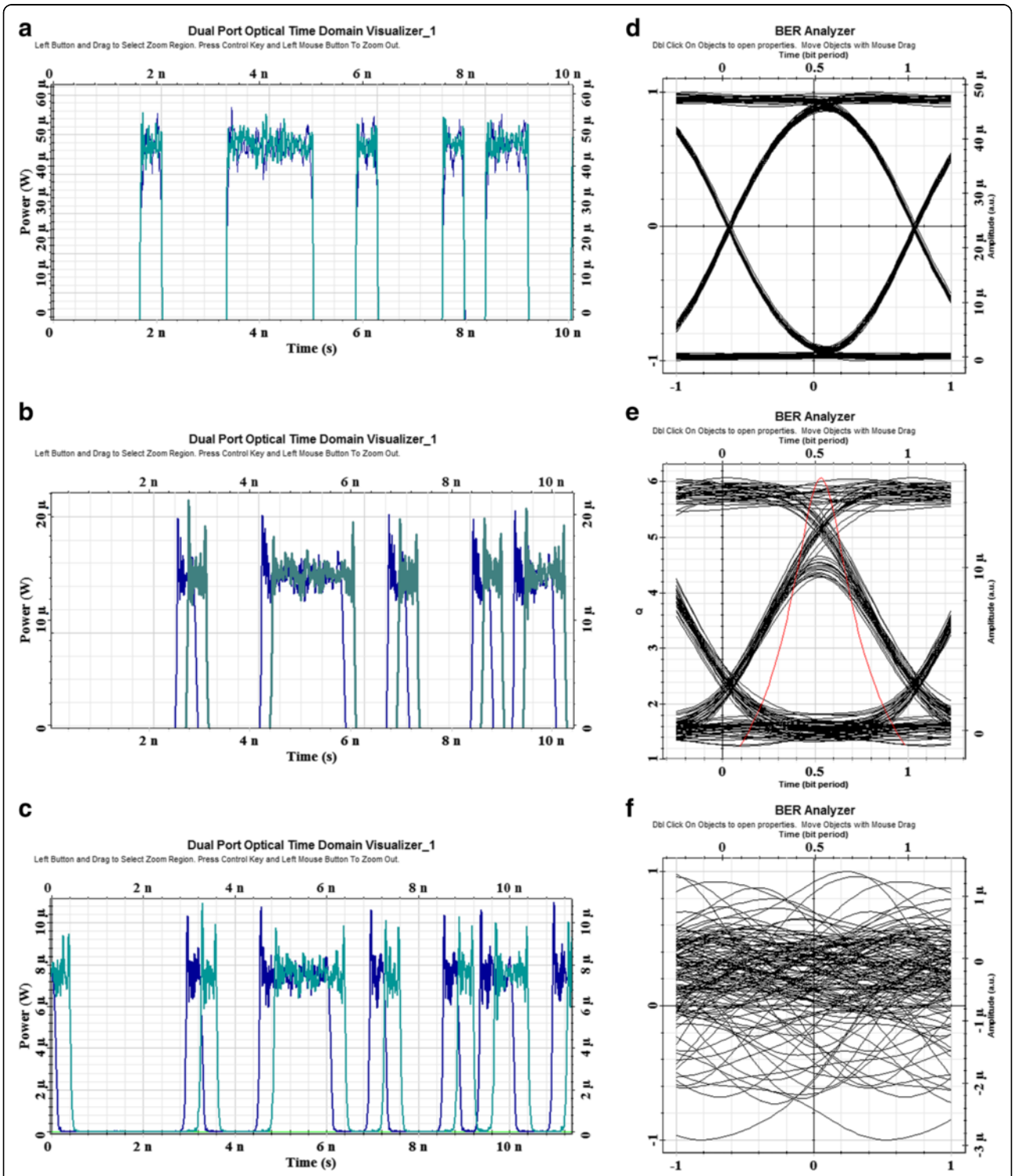

Fig. 5 Evaluation of code shift and corresponding eye diagrams (**a**) L = 0 km (**b**) L = 25 km (**c**) L = 40 km (**d**) Eye at L = 0 km (**e**) Eye at L = 25 km and (**f**) Eye at L = 40 km

16 times the input RF LO. These sidebands are modulated with the 2.5 Gb/s NRZ data of length 2^{7-1} using an intensity modulator and then combined with the unmodulated +12th (195.145 THz) order sideband as shown in Fig. 4(a). This field is transported from CS to the BS1 over a 25 km SMF with 0.2 dB/km attenuation coefficient and 16.75 ps/nm-km dispersion coefficient. The dispersion slope and PMD coefficient of the fiber is 0.075 ps/nm^2.km and 0.05 ps/√km. At the BS1, before the photo detection process another FBG with 10 GHz bandwidth is tuned to reflect the unmodulated tone located at 195.145 THz which is reused for carrying the 2.5 Gb/s NRZ upstream data over 25 km SMF from BS1 to CS. The upstream data modulated spectrum from the BS1 is shown in Fig. 4(c). The losses of both the links are compensated using an optical amplifier with a noise Figure of 4. Similarly at the lower sideband spectra, a 2.5 Gb/s NRZ data modulated over −4th (195.085 THz) and −20th (195.025 THz) order sidebands are combined with the unmodulated −12th (195.055 THz) order sideband and then transmitted from CS to BS2 over 25 km SMF. The data modulated spectrum for the BS2 is shown in Fig. 4(b). At the BS2 prior to the photo detection, the tone corresponding to 195.055 THz is separated using the FBG and reused for the 2.5 Gb/s upstream data transmission to the CS. The upstream data modulated spectrum from the BS2 is shown in Fig. 4(d). The downstream signal received at the both the BSs are detected using a PIN photo-detector with 0.7 A/W responsivity, 100e^{-24} W/Hz thermal power density and 10 nA dark current and then passed through a band pass filter having a centre frequency of 60 GHz with a bandwidth 1.5 times the bitrate so as to select the data modulated 60 MM-Wave signal. This signal is then demodulated and then passed through a low pass filter with a bandwidth of 0.75 times the bitrate. The upstream data received at the CS is detected using the PIN detector and demodulated. BER performance of both downstream and the upstream are measured by varying the received optical power using an optical attenuator.

In the downstream, compared to the back-to-back case, the BER performance is degraded due to the dispersion induced RF power fading and the bit-walk off effect on the dual tone modulation. Since the dispersion causes the data on each sideband to undergo different time and phase shift, the data bits walk off from each other as the function of fiber length L [23]. The code shift between the sidebands is measured for various length of the fiber and it is shown in Fig. 4. From the Fig. 5(a)-(c), it is clear that the codes on the sidebands are exactly coinciding when the fiber length L = 0, the shift is acceptable when L = 25 km and the data completely walks off when L = 40 km and beyond. The Eye diagrams of the corresponding lengths are

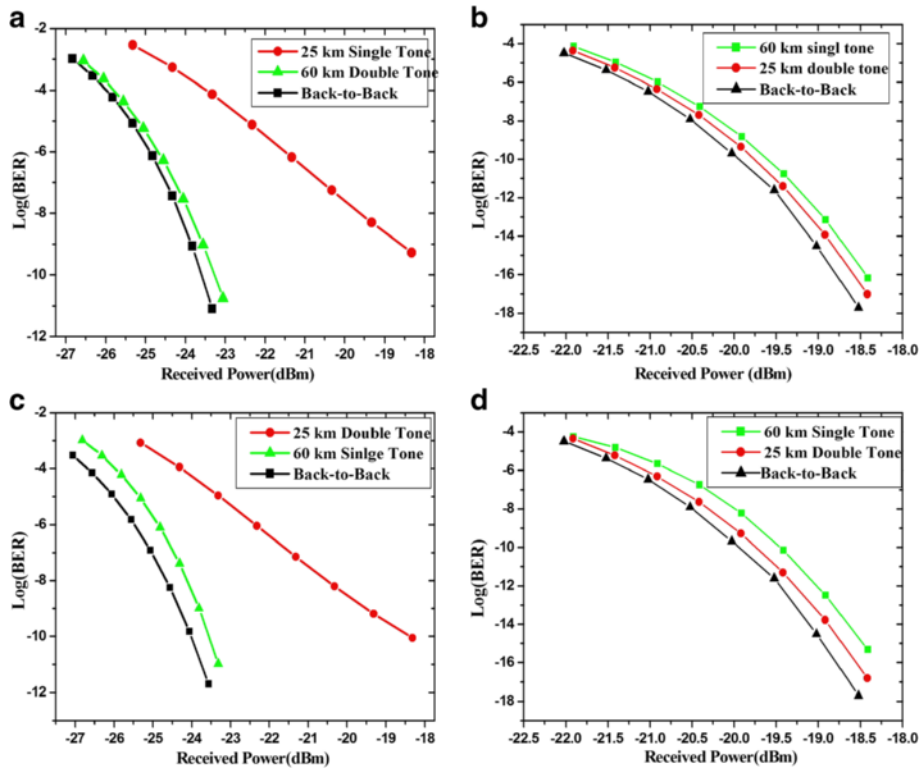

Fig. 6 BER performance at (**a**) BS1 downlink (**b**) BS 1 uplink (**c**) BS 2 downlink (**d**) BS 2 uplink

also shown in Fig. 5(d)-(f). As the code shift is more the eye completely closes. Hence the transmission distance is limited to 25 km in case of the double sideband data modulation with a power penalty of 5 dB at 10^{-9} BER for the both BSs downlink. The BER performance against the received power for BS1 and BS2 are shown Fig. 6(a) and 5(c) respectively. But the BER performance of the upstream transmission is very close to the back-to-back (B-t-B) BER due to the fact that there is no modulated RF carrier and hence no power fading and bit walk off effect. Therefore, the dispersion induced power penalty at the 10^{-9} BER for the upstream transmission is less than 0.3 dB. The transmission distance can be increased by modulating the data over only one of the sidebands. As the data modulated over only one sideband, the effect of dispersion induced power fading and the bit walk off effects are eliminated. Hence the transmission distance of the scheme is extended to 60 km. Further increase in the transmission distance is attributed to the pulse broadening due to the dispersion. The BER performance of the single tone modulation is compared with B-t-B case and double tone modulation and is shown in the Fig. 6(a)-(d). The dispersion induced power penalty for the single tone modulation is less than 0.5 dB for the down and upstream at 10^{-9} BER.

Conclusion

A new approach for generating the frequency dual 16-tupling is proposed and demonstrated using parallel configuration of two stage cascaded MZMs. This system simultaneously supported two base stations with bidirectional data transmission between BS and CS by wavelength reuse without additional requirements; hence costs of the BSs are also reduced significantly. Transmission Performance is evaluated for both double tone and single tone modulation formats. The simulation result showed 5 dB dispersion induced power penalty in the downstream data transmission and less than 0.3 dB for the upstream transmission over 25 km SMF at the BER of 10^{-9} for the double tone data modulation. With the single tone modulation transmission, the link distance is extended to 60 km with dispersion induced power penalty less than 0.5 dB for both upstream and downstream.

Acknowledgements
The authors thankfully acknowledge the Department of Science and Technology (DST), New Delhi for their Fund for Improvement of S&T Infrastructure in Universities and Higher Educational Institutions – (FIST) grant through the order No.SR/FST/College-061/2011(C) to procure the Optiwave suite Simulation tools.

Authors' contribution
KEM has worked out the mathematical derivations of the proposed system and carried out all the simulation works. ASR has developed the concept and involved in the manuscript preparation. Both authors read and approved the final manuscript.

Competing interests
The authors declare that they have no competing interests.

Author details
[1]University VOC College of Engineering, University VOC, Thoothukudi, Tamilnadu 630003, India. [2]A.C.College of Engineering and Technology, Karaikudi, Tamilnadu 630004, India.

Received: 21 July 2016 Accepted: 9 November 2016
Published online: 22 November 2016

References

1. Capmany, J., Novak, D.: Microwave photonics combines twoworlds. Nat. Photonics **1**, 319–330 (2007)
2. Qi, G., Yao, J.P., Seregelyi, J., Paquet, S., Belisle, C.: Generation and distribution of wide-band continuously tunable millimeter wave signal with an optical external modulation technique. IEEE Trans. Microwave Theory Tech. **53**, 3090–3097 (2005)
3. O'Rcilly, J.J., Lane, P.M., Heidemann, R., Hofstetter, R.: Opical generation of verynarrow linewidth Millimeter wave signals. Electron. Lett **28**(25), 2309–2311 (1992)
4. Wang, Q., Rideout, H., Zeng, F., Yao, J.P.: Millimeter-Wave frequency tripling based on four-wave mixing in a semiconductor optical amplifier. IEEE Photon. Technol. Lett. **18**(23), 2460–2462 (2006)
5. Lin, C.T., Shih, P.T., Chen, J., Xue, W.Q., Peng, P.C., Chi, S.: Optical millimeter wave signal generation using frequency quadrupling technique and no optical filtering. IEEE Photon. Technol. Lett. **20**(12), 209–211 (2008)
6. Mohamed, M., Zhang, X., Hraimel, B., Wu, K.: Analysis of frequency quadrupling using a singleMach-Zehnder modulator for millimeter-wavegeneration and distribution over fiber systems. Opt Express **16**(14), 10786–10802 (2008)
7. Yu, S., Gu, W., Yang, A., Jiang, T., Wnag, C.: A Frequency quadrupling optical mm-Wave generation for hybrid fiber-wireless systems. IEEE J. Sel. Areas Commun/Supplement- Part 2 **31**(12), 797–803 (2013)
8. Mohamed, M., Zhang, X., Hraimel, B., Wu, K.: Frequency sixupler for millimeter-wave over fiber systems. Opt Express **15**, 10141–10151 (2008)
9. Ma, J., Xin, X., Yu, J., Yu, C., Wnag, K., Huang, H., Rao, L.: Optical millimeter wave generated by octupling the frequency of the local oscillator. J. Opt. Netw. **7**, 837–845 (2008)
10. Zhu, Z., Zhao, S., Li, Y., Chu, X., Wnag, X., Zhao, G.: A radio over fiber system with frequency 12-Tupling optical millimeter wave generation to overcome chromatic dispersion. Quantum Electron. Lett. **49**, 919–922 (2013)
11. Chen, H., Ning, T., Jian, W., Pei, L., Li, J.: D-band millimeter-wave generator based on a frequency 16-tupling feedforward modulation technique. Opt. Eng. **52**, 0761041–0761044 (2013)
12. Zhu, Z., Zhao, S., Chu, X., Dong, Y.: Optical generation of millimeter – wave signals via frequency 16-tupling without an optical filter. Opt. Commun. **354**, 40–47 (2015)
13. Hu, J.H., Huang, X.G., Xie, J.L.: A full-duplex radio-over-fiber systems based on dual quadrupling-frequency. Opt. Commun. **284**, 729–734 (2011)
14. Yang, K., Huang, X.G., Zhu, J.H., Fang, W.J.: Transmission of 60 GHz wired/wireless based on full-duplex radio-over-fiber using dual-sextupling frequency. IET Commun. **6**, 2900–2906 (2012)
15. Cheng, G., Guo, B., Liu, S., Fang, W.: A novel full-duplex radio-over-fiber systems based on dual octupling-frequency for 82 GHz W-band radio frequency and wavelength reuse for uplink connection. Optik **125**, 4072–4076 (2014)
16. Zhao, Z., Wen, Y., Zhang, H.: Simplified optical millimeter wave generation conFigureuration by frequency quadrupling using two cascaded Mach-Zehnder modulators. Opt Lett **34**, 3250–3252 (2009)
17. Qin, Y., Sun, J.: Frequency sextupling technique using two cascaded dual-electrode Mach-Zehnder modulators interleaved with Gaussian band pass filter. Opt. Commun. **285**, 2911–2916 (2012)
18. Chen, Y., Wen, A., Shang, L.: Analysis of an optical mm-wave generation scheme with frequency octupling using two cascaded Mach-zehnder modulators. Opt. Commun. **283**, 4933–4941 (2010)
19. Chen, Y., Wen, A., Yin, X., Shang, L.: A photonic mm-wave frequency sextupler using an Inegrated Mach-Zehnder modulator with three arms. Fiber Integr. Opt. **31**, 196–207 (2012)
20. Chen, Y., Wen, A., Guo, J., Shang, L., Wang, Y.: A novel optical mm-wave generation scheme based on three parallel Mach-Zehnder modulators. Opt. Commun. **284**, 1159–1169 (2011)

21. Shang, L., Wen, A., Li, B., Wang, T., Chen, Y., Li, M.: A filterless optical millimeter wave generation based on frequency octupling. Optik **123**, 1183–1186 (2012)
22. Hasan, M., Hall, T.J.: A Photonic frequency octo-tupler with reduced RF drive power and extended spurious sideband suppression. Opt. Laser Technol. **81**, 115–121 (2016)
23. Zhoua, M., Ma, J.: Influence of fiber dispersion on the transmission performance of a quadruple frequency optical millimeter wave with two signal modulation format. Opt Swtiching Netw **9**, 343–350 (2012)